

# 基于声光调制模式切换的宽重复频率微秒脉冲光纤放大器

胡梁<sup>1,2</sup>, 钱勇<sup>2</sup>, 李培丽<sup>1</sup>, 周军<sup>1,2,3\*</sup><sup>1</sup>南京邮电大学电子与光学工程学院、柔性电子(未来技术)学院, 江苏南京 210023;<sup>2</sup>南京先进激光技术研究院, 江苏南京 210038;<sup>3</sup>中国科学院上海光学精密机械研究所, 上海 201800

**摘要** 设计并实现了重复频率在 10 Hz~10 kHz 可调的 1550 nm 微秒矩形脉冲光纤放大器。该光纤放大器采用双级主振荡功率放大(MOPA)全光纤结构,采用声光调制器对信号光进行调制,通过对泵浦驱动和信号光调制的脉冲波形及时序进行优化,实现了峰值功率为 30 W、脉冲宽度为 10  $\mu$ s~1 ms、重复频率在 10 Hz~10 kHz 范围可调的微秒矩形脉冲放大激光输出。通过优化信号光脉冲和泵浦脉冲时序有效抑制了光纤放大过程中的放大自发辐射,通过对信号光的脉冲波形进行预整形获得了较好的微秒矩形脉冲输出。

**关键词** 光学器件; 光放大器; 微秒脉冲; 铟-镱共掺光纤; 声光调制器; 主振荡功率放大器

中图分类号 TN722

文献标志码 A

DOI: 10.3788/CJL221518

## 1 引言

人眼安全波段的 1.5  $\mu$ m 脉冲光纤放大器是脉冲光纤激光技术研究的热点之一<sup>[1-4]</sup>。不同脉冲宽度的光学放大器应用于不同的场合,如:飞秒、皮秒光纤放大器应用于激光测距<sup>[5-6]</sup>;纳秒光纤放大器应用于激光雷达<sup>[7]</sup>;微秒光纤放大器由于峰值功率密度相对较低,热效应明显且热损伤小,常常应用于激光钻孔<sup>[8]</sup>、激光着色<sup>[9]</sup>、生物医学<sup>[10]</sup>等领域。相较于纳秒光纤放大器,由于放大期间的脉冲波形变陡以及低重复频率下显著增大的放大自发辐射(ASE),微秒脉冲光纤放大器的研究更具挑战性。

调 Q 光纤激光器和基于主振荡功率放大(MOPA)结构的光纤放大器是实现微秒脉冲光的两种可行方案。2021 年,西北大学的陈双成<sup>[11]</sup>利用基于 Sagnac 环的调 Q 光纤激光器实现了脉冲宽度为 2.91~7.17  $\mu$ s、重复频率在 39.47~58.57 kHz 范围可调的微秒脉冲,其峰值功率为 3.01 mW。2022 年,王天祺等<sup>[12]</sup>利用石墨烯全光调制的主/被动调 Q 光纤激光器实现了脉冲宽度为 5.32~10.3  $\mu$ s、重复频率在 18.7~47.17 kHz 范围可调的微秒脉冲,其峰值功率为 2~8 mW。虽然调 Q 光纤激光器结构简单,但其脉冲宽度和重复频率可调范围小,峰值功率低,因此,脉冲宽度和重复频率可调范围大、峰值功率高的 MOPA 结构微秒脉冲光纤放大器受到了一些学者的青睐。

2020 年,土耳其光纤激光系统和技术公司的 Pavlova 等<sup>[13]</sup>利用三级 MOPA 结构实现了工作波长为 1550 nm、脉冲宽度为 10~100  $\mu$ s、重复频率在 50 Hz~10 kHz 可调的矩形微秒脉冲,其峰值功率为 32 W。为了解决显著增长的 ASE 光,Pavlova 等采用 1560 nm 种子源作为辅助种子源,但采用两个种子源和空间滤波方案增加了系统复杂度及成本,且空间滤波后仍有 1560 nm 光残留。2022 年,俄罗斯科学研究所应用物理研究所的 Koptev 等<sup>[10]</sup>利用大模场掺铟光纤实现了脉冲宽度为 200  $\mu$ s~5 ms、峰值功率为 28.6 W 的矩形脉冲输出,但其重复频率为 100 Hz~2.5 kHz,可调范围小,矩形脉冲宽度为亚毫秒级。

笔者采用脉冲泵浦的全光纤 MOPA 结构,通过设置声光调制器(AOM)的两种工作模式,实现了工作波长为 1550 nm、峰值输出功率为 30 W、脉冲宽度为 10  $\mu$ s~1 ms、重复频率在 10 Hz~10 kHz 范围可调的矩形脉冲光纤放大器。通过优化信号光和泵浦光的时序及脉冲宽度抑制了 ASE 快速增长,通过对信号光脉冲波形进行预整形解决了微秒脉冲光纤放大过程中瞬态增益效应导致的波形畸变问题,最终获得了较好的矩形脉冲激光输出。

## 2 实验装置与方案

实验装置如图 1 所示。整个实验装置主要由信号

收稿日期: 2022-12-12; 修回日期: 2023-02-12; 录用日期: 2023-03-01; 网络首发日期: 2023-03-09

基金项目: 江苏省科技成果转化专项资金项目(BA2022010)

通信作者: junzhousd@mail.siom.ac.cn

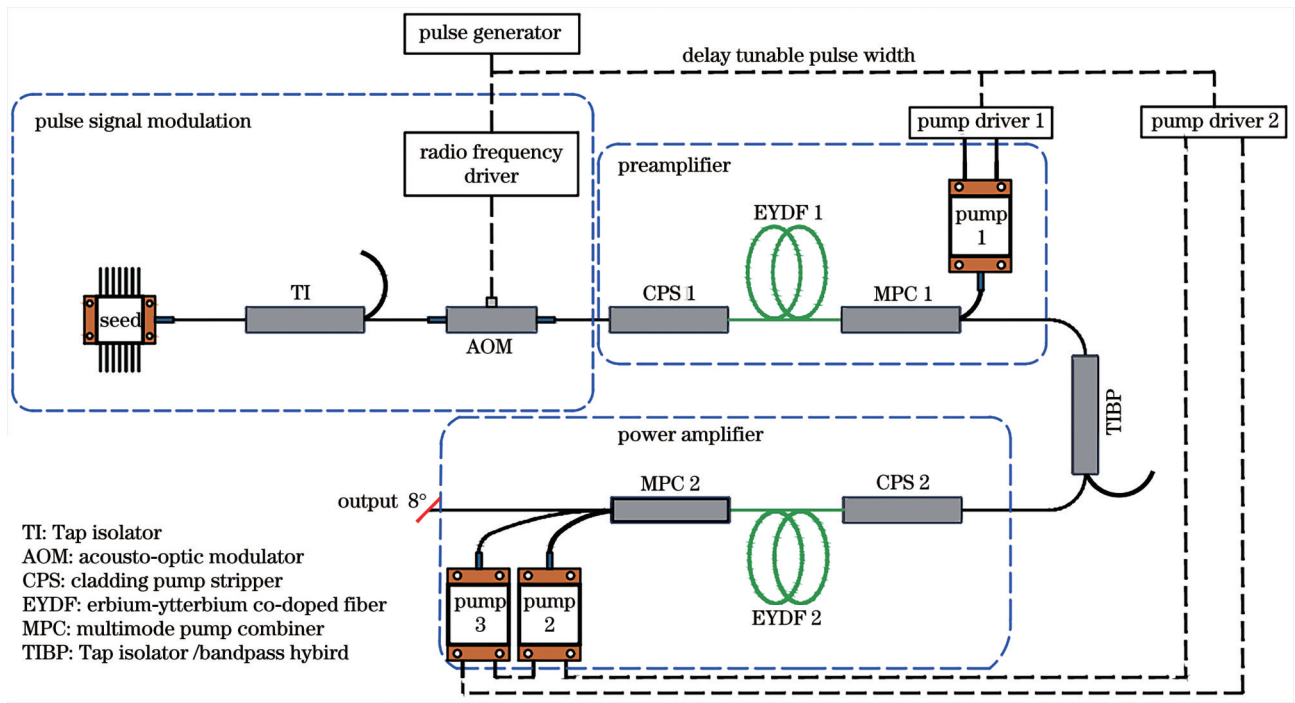


图 1 实验装置图

Fig. 1 Experimental setup schematic

光脉冲调制模块、预放大器、功率放大器、脉冲信号驱动及控制模块组成。

信号光脉冲调制模块包含连续种子源(中心波长为 1549.7 nm,最大输出光功率为 0.038 W,线宽小于 1 MHz,边模抑制比为 58 dB)、Tap 隔离器、声光调制器(SGTF80-1550-1P,插入损耗为 2.2 dB,移频频率为 80 MHz,光脉冲上升时间小于 0.05 μs)。声光调制器的脉冲上升时间远短于信号光脉冲 10 μs 的持续时间,可以精确控制信号光脉冲波形。

预放大器包括双包层钕镱共掺增益光纤(Nuferm, PM-EYDF-12/130,长度为 2.4 m)、泵浦激光二极管(泵浦波长为 940 nm,最大光功率为 10 W)、多模泵浦合束器(MPC)、包层光滤除器(CPS)。包层光滤除器用于吸收光路中多余的 940 nm 泵浦光,防止损坏器件。预放大器后接 Tap 带通滤波隔离器(分束比为 999:1)以滤除宽带 ASE,同时通过 Tap 端对预放大器进行监测。

功率放大器包括双包层钕镱共掺增益光纤(Nuferm, PM-EYDF-12/130,长为 3.8 m)、泵浦激光二极管(泵浦波长为 940 nm,最大光功率为 80 W)、多模泵浦合束器、包层光滤除器。

激光二极管及其驱动器在产生泵浦脉冲时存在几十微秒的上升沿时间,导致泵浦能量传递给信号光脉冲时存在几十微秒的上升沿时间。当信号光脉冲宽度小于 100 μs 时,上升沿时间与脉冲宽度的比值过大,导致光脉冲波形发生畸变。因此,设置声光调制器工作在两种模式:1)直流调制驱动模式(模式 1),该模式对应输出信号的光脉冲宽度在 100 μs~1 ms 之间;2)脉冲调制驱动模式(模式 2),该模式下种子源连续输出光被调制成脉冲光,对应输出信号光脉冲宽度在 10~100 μs 之间。声光调制器射频驱动、预放大器泵浦驱动、功率放大器泵浦驱动的工作模式如表 1 所示,三者脉冲时序可实现精确的同步控制,且脉冲宽度可调。

表 1 声光调制器射频驱动和泵浦驱动的工作模式

Table 1 Working mode of acousto-optic modulator (AOM) radio frequency (RF) driver and pump driver

Controlled device	Working mode	
	Mode 1 (pulse width of 100 μs~1 ms, repetition frequency of 10 Hz~1 kHz)	Mode 2 (pulse width of 10~100 μs, repetition frequency of 1~10 kHz)
AOM driver	1) Direct current mode 2) Amplitude is adjustable	1) Pulse mode 2) Waveforms can be simulated and edited
Preamplifier pump driver	1) Rectangular pulse mode 2) Amplitude and pulse width are adjustable	1) Rectangular pulse mode 2) Amplitude and pulse width are adjustable
Power amplifier pump driver	1) Rectangular pulse mode 2) Amplitude and pulse width are adjustable	1) Rectangular pulse mode 2) Amplitude and pulse width are adjustable

声光调制器射频驱动、预放大器泵浦驱动、功率放

大器泵浦驱动的脉冲时序如图 2 所示

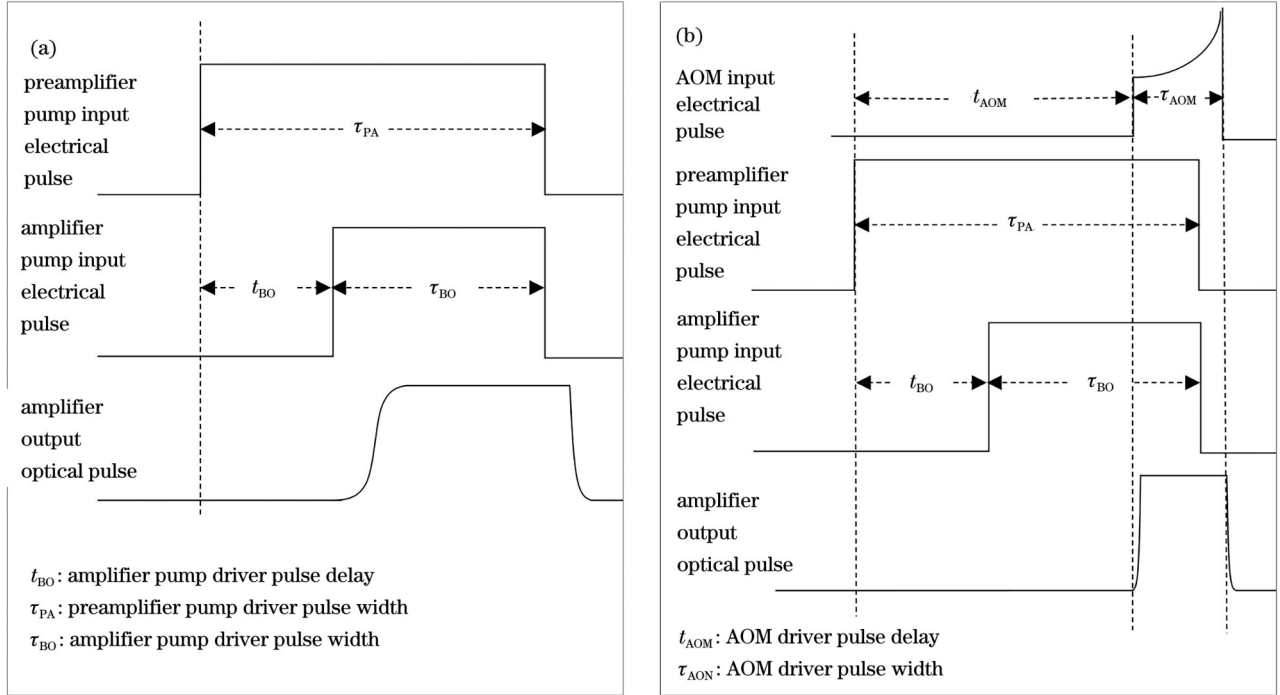


图 2 声光调制器驱动和泵浦驱动脉冲时序。(a)模式 1;(b)模式 2

Fig. 2 AOM driver and pump driver pulse timing. (a) Mode 1; (b) mode 2

钇-镱共掺系统的能级结构如图 3 所示。由于  $Er^{3+}$

的  $^4I_{11/2}$  能级和  $^4I_{13/2}$  能级之间的弛豫时间较长(0.1~10  $\mu s$ ), 而且  $Yb^{3+}$  的  $^2F_{5/2}$  能级和  $Er^{3+}$  的  $^4I_{11/2}$  能级之间的交叉弛豫时间长, 钇-镱共掺光纤的布居数反转缓慢, 需泵浦 100  $\mu s$  以上才能达到稳态<sup>[14-15]</sup>, 因此, 实验中采用预泵浦技术同时优化预泵浦持续时间(泵浦和信号光之间的延时), 以获得最佳的矩形脉冲。

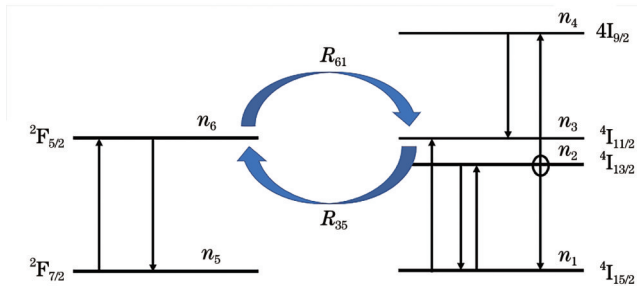


图 3 钇-镱共掺系统的能级结构

Fig. 3 Energy-level diagram of erbium-ytterbium co-doped system

### 3 实验结果与分析

为了抑制 ASE 的快速增长, 笔者优化了信号光脉冲和泵浦驱动的时序、脉宽设置。脉冲光纤放大器声光调制器射频驱动、预放大器泵浦驱动、功率放大器泵浦驱动的脉冲时序和脉冲宽度设置如表 2 所示。

表 2 声光调制器射频驱动和泵浦驱动的脉冲时序及脉冲宽度设置

Table 2 Pulse timing and pulse width settings of acousto-optic modulator (AOM) radio frequency (RF) driver and pump driver

Mode	Repetition frequency $f_{rep}/Hz$	Pulse width $\tau/\mu s$	AOM setting		Preamplifier pump setting		Amplifier pump setting	
			Trigger delay $t_{AOM}/\mu s$	Pulse width $\tau_{AOM}/\mu s$	Trigger delay $t_{PA}/\mu s$	Pulse width $\tau_{PA}/\mu s$	Trigger delay $t_{BO}/\mu s$	Pulse width $\tau_{BO}/\mu s$
1	10	1000			0	1500	390	1100
	1000	100			0	400	280	110
2	1000	10	390	11	0	300	140	160
	10000	10	70	11	0	80	18	60

功率放大器输出信号光脉冲波形图如图 4 所示。从图 4 可以看出, 输出信号光脉冲波形基本为矩形。设置声光调制器工作于模式 1, 通过优化两级光纤放大器泵浦驱动时序及脉冲宽度得到的典型结果

如图 4(a) 和图 4(b) 所示。由于泵浦脉冲存在约 100  $\mu s$  的上升沿时间, 当脉冲宽度减小到 100  $\mu s$  时, 脉冲波形开始有所畸变。设置声光调制器工作于模式 2, 由于脉冲光纤放大器的瞬态增益效应, 脉冲前沿的放

大对后沿放大有所抑制,矩形脉冲的前沿增益大于后沿增益,因此脉冲峰值向前沿方向移动,脉冲波形前沿变陡<sup>[16]</sup>。为了获得较好的矩形脉冲放大输出,利用声光调制器对输入信号光脉冲波形进行预整形,同时优化声光调制器的参数设置,在 1 kHz 和 10 kHz 重复频率

时均获得了较好的 10  $\mu\text{s}$  矩形脉冲输出,如图 4(c)和图 4(d)所示。

不同脉冲重复频率和脉冲宽度下,预放大器、功率放大器输出光峰值功率和光-光转换效率如表 3 所示。

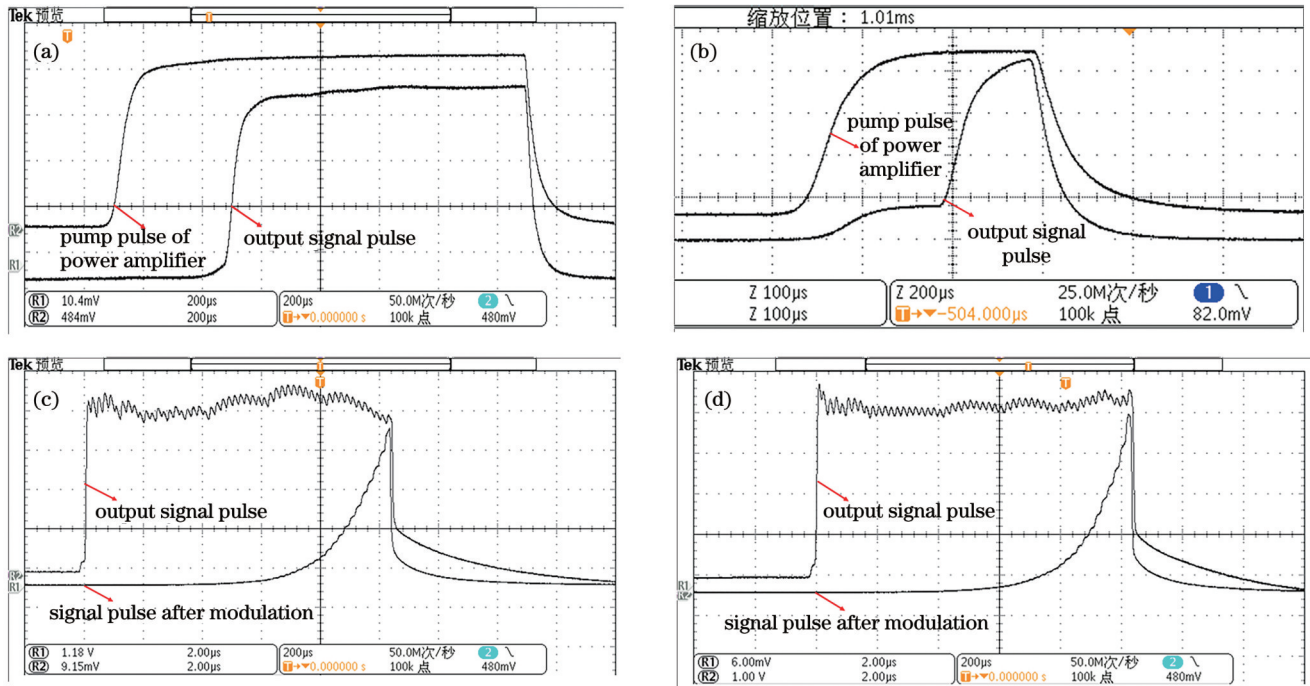


图 4 功率放大器信号光脉冲波形图。(a)重复频率 10 Hz,脉冲宽度 1 ms;(b)重复频率 1 kHz,脉冲宽度 100  $\mu\text{s}$ ;(c)重复频率 1 kHz,脉冲宽度 10  $\mu\text{s}$ ;(d)重复频率 10 kHz,脉冲宽度 10  $\mu\text{s}$

Fig. 4 Power amplifier signal pulse waveform. (a) Repetition frequency of 10 Hz, pulse duration of 1 ms; (b) repetition frequency of 1 kHz, pulse duration of 100  $\mu\text{s}$ ; (c) repetition frequency of 1 kHz, pulse duration of 10  $\mu\text{s}$ ; (d) repetition frequency of 10 kHz, pulse duration of 10  $\mu\text{s}$

表 3 脉冲光纤放大器输出参数  
Table 3 Pulsed fiber amplifier output parameters

Mode	Repetition frequency $f_{\text{rep}} / \text{Hz}$	Pulse duration $\tau / \mu\text{s}$	Peak power after modulation $P_{\text{IN}} / \text{W}$	Peak power of preamplifier $P_{\text{PA}} / \text{W}$	Peak power of power amplifier $P_{\text{BO}} / \text{W}$	Optical conversion efficiency $\eta / \%$
1	10	1000	0.02025	1.50	30.90	34.68
	100	1000	0.02025	1.55	30.50	34.23
	1000	100	0.02025	1.56	30.02	33.69
2	1000	10	0.03060	2.07	30.01	19.50
	2000	10	0.03035	2.08	30.05	21.95
	10000	10	0.03190	2.16	30.07	24.19

从表 3 可以看出,脉冲光纤放大器设置在不同重复频率、不同脉冲宽度时,放大输出激光的峰值功率均可达到 30 W。通过计算发现,设置声光调制器工作于模式 1 时,预放大器增益达到 18.7 dB,功率放大器增益达到 12.84 dB,脉冲光纤放大器总增益达到 31.7 dB,光-光转换效率为 33.69%~34.68%,优于参考文献 [10] 中 26% 的光-光转换效率。设置声光调制器工作于模式 2 时,预放大器增益达到 18.3 dB,功率放大器增益达到 11.44 dB,脉冲光纤放大器总增益达到

29.75 dB。当脉冲宽度为 10  $\mu\text{s}$  时,随着重复频率从 1 kHz 增大到 10 kHz,光-光转换效率从 19.50% 逐渐增大到 24.19%。这是因为,一方面,随着脉冲重复频率的不断增大,两个相邻脉冲间隔变短,ASE 积累时间缩短,有利于信号光功率的增大;另一方面,保持脉冲宽度不变时,随着脉冲重复频率不断增大,脉冲占空比不断增加,单位时间内的脉冲数量不断增多,从而使得单位时间内吸收的泵浦光能量增加。

脉冲光纤放大器在不同重复频率和不同脉冲宽度

下的输出光谱图如图 5 所示。当设置声光调制器工作于模式 1 时,由于已经优化信号光脉冲和泵浦脉冲的时序(抑制 ASE 增长),光谱边模抑制比接近 55 dB,基本没有 ASE 产生。当设置声光调制器工作于模式 2

时,光谱边模抑制比为 25 dB。这是因为信号光的脉冲宽度较窄,单个信号光脉冲过后单个泵浦脉冲多余的部分能量继续进行离子间能量转换,ASE 迅速累积,导致光谱边模抑制比有所下降。

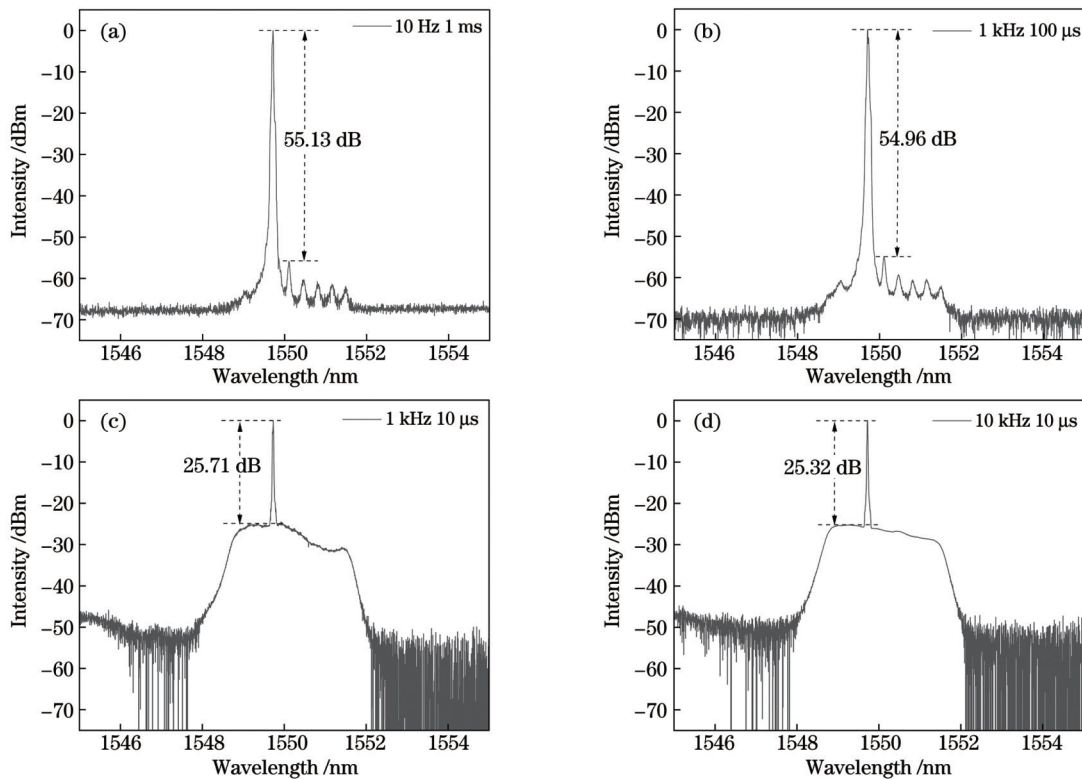


图 5 功率放大器输出光谱图(光谱分辨率为 0.02 nm)。(a)重复频率 10 Hz,脉冲宽度 1 ms;(b)重复频率 1 kHz,脉冲宽度 100  $\mu$ s;(c)重复频率 1 kHz,脉冲宽度 10  $\mu$ s;(d)重复频率 10 kHz,脉冲宽度 10  $\mu$ s

Fig. 5 Power amplifier output spectrum (spectral resolution is 0.02 nm). (a) Repetition frequency of 10 Hz and pulse duration of 1 ms; (b) repetition frequency 1 kHz and pulse duration of 100  $\mu$ s; (c) repetition frequency of 1 kHz and pulse duration of 10  $\mu$ s; (d) repetition frequency of 10 kHz and pulse duration of 10  $\mu$ s

## 4 结 论

研制了一种基于信号光声光调制的双级全光纤 MOPA 结构 1550 nm 微秒矩形脉冲光纤放大器。通过对脉冲信号进行时序控制和波形预整形,解决了脉冲光纤放大器 ASE 快速增长和瞬态效应问题;通过设置声光调制器工作于两种不同模式解决了脉冲宽度变窄导致的波形畸变问题,最终实现了脉冲宽度为 10  $\mu$ s~1 ms、重复频率在 10 Hz~10 kHz 大范围内可调的矩形光脉冲,脉冲峰值功率为 30 W。该微秒脉冲光纤放大器峰值功率高,脉冲宽度和重复频率理论上可以实现更大范围可调,在激光钻孔、激光着色、生物医学等领域具有广阔的应用前景。

## 参 考 文 献

- [1] 王丽莎, 孙松松, 闫炜, 等. L 波段可切换双波长高能脉冲光纤激光器[J]. 红外与激光工程, 2021, 50(7): 20200370.  
Wang L S, Sun S S, Yan W, et al. L-band switchable dual-wavelength, high-energy pulsed fiber laser[J]. Infrared and Laser Engineering, 2021, 50(7): 20200370.
- [2] Yao G, Zhao Z G, Liu Z J, et al. High repetition rate actively mode-locked Er: fiber laser with tunable pulse duration[J]. Chinese Optics Letters, 2022, 20(7): 071402.
- [3] Wu Q, Wang Y Z, Huang W C, et al. MXene-based high-performance all-optical modulators for actively Q-switched pulse generation[J]. Photonics Research, 2020, 8(7): 1140-1147.
- [4] 王增超, 孟阔, 陈恺, 等. 基于宽带啁啾光纤光栅掺铒光纤激光啁啾脉冲放大方法研究[J]. 中国激光, 2021, 48(11): 1101002.  
Wang Z C, Meng K, Chen K, et al. Research on erbium-doped fiber lasers using chirped pulse amplification method based on broadband chirped fiber grating[J]. Chinese Journal of Lasers, 2021, 48(11): 1101002.
- [5] 薛睿, 武子铃, 董佳琦, 等. 基于电控光学采样的飞秒激光距离测量系统[J]. 光学学报, 2023, 43(3): 0312002.  
Xue R, Wu Z L, Dong J Q, et al. Femtosecond laser distance measurement based on electronically controlled optical sampling[J]. Acta Optica Sinica, 2023, 43(3): 0312002.
- [6] 龙明亮, 邓华荣, 张海峰, 等. 1 kHz 重复频率多脉冲皮秒激光器研制及其空间碎片激光测距应用[J]. 光学学报, 2021, 41(6): 0614001.  
Long M L, Deng H R, Zhang H F, et al. Development of multiple pulse picosecond laser with 1 kHz repetition rate and its application in space debris laser ranging[J]. Acta Optica Sinica, 2021, 41(6): 0614001.
- [7] Yun J, Gao C X, Zhu S L, et al. High-peak-power, single-mode, nanosecond pulsed, all-fiber laser for high resolution 3D imaging LIDAR system[J]. Chinese Optics Letters, 2012, 10(12): 121402-

- 121404.
- [8] Tu J, Paleocrassas A G, Reeves N, et al. Experimental characterization of a micro-hole drilling process with short microsecond pulses by a CW single-mode fiber laser[J]. *Optics and Lasers in Engineering*, 2014, 55: 275-283.
- [9] 张龙达, 李好发, 安丰硕, 等. 基于 Elman 神经网络的不锈钢微秒激光着色预测[J]. *中国激光*, 2022, 49(8): 0802010.  
Zhang L D, Li H F, An F S, et al. Elman-neural-network based prediction of microsecond laser coloring on stainless steel[J]. *Chinese Journal of Lasers*, 2022, 49(8): 0802010.
- [10] Koptev M Y, Morozov A N, Shatilova K V, et al. All-fiber high-power erbium-doped laser system generating optical pulses with a duration of 200  $\mu$ s to 5 ms for fractional photo-rejuvenation[J]. *Applied Optics*, 2022, 61(16): 4851-4856.
- [11] 陈双成. 波长可切换可调谐掺铒脉冲光纤激光器的研究[D]. 西安: 西北大学, 2021: 29-32.  
Chen S C. The study of wavelength switchable and tunable erbium-doped pulsed fiber laser[D]. Xi'an: Northwest University, 2021: 29-32.
- [12] 王天祺, 李对对, 刘贝贝, 等. 基于石墨烯全光调制的主/被动调 Q 光纤激光器(特邀)[J]. *光子学报*, 2022, 51(10): 1014004.  
Wang T Q, Li D D, Liu B B, et al. Active-passive Q-switched fiber laser based on graphene all-optical modulation(invited) [J]. *Acta Photonica Sinica*, 2022, 51(10): 1014004.
- [13] Pavlova S, Yagci M E, Eken S K, et al. High power microsecond fiber laser at 1.5  $\mu$ m[J]. *Optics Express*, 2020, 28(12): 18368-18375.
- [14] 吕晓英, 韩群, 刘铁根. 高功率脉冲抽运 Er-Yb 共掺光纤放大器的理论研究[J]. *中国激光*, 2014, 41(6): 0602003.  
Lü X Y, Han Q, Liu T G. Theoretical investigation of high-power pulse-pumped Er-Yb codoped fiber amplifiers[J]. *Chinese Journal of Lasers*, 2014, 41(6): 0602003.
- [15] Canat G, Mollier J C, Bouzina J P, et al. Dynamics of high-power erbium-ytterbium fiber amplifiers[J]. *Journal of the Optical Society of America B*, 2005, 22(11): 2308-2318.
- [16] 楼祺洪, 周军, 孔令峰, 等. 高功率脉冲双包层光纤激光器的新进展[J]. *量子电子学报*, 2005, 22(4): 510-515.  
Lou Q H, Zhou J, Kong L F, et al. Recent progress of high power pulsed double cladding fiber lasers[J]. *Chinese Journal of Quantum Electronics*, 2005, 22(4): 510-515.

## Wide Repetition Frequency Microsecond Pulsed Fiber Amplifier Based on Acousto-Optic Modulating Mode Switching

Hu Liang<sup>1,2</sup>, Qian Yong<sup>2</sup>, Li Peili<sup>1</sup>, Zhou Jun<sup>1,2,3\*</sup>

<sup>1</sup>College of Electronic and Optical Engineering & College of Flexible Electronics (Future Technology), Nanjing University of Posts and Telecommunications, Nanjing 210023, Jiangsu, China;

<sup>2</sup>Nanjing Institute of Advanced Laser Technology, Nanjing 210038, Jiangsu, China;

<sup>3</sup>Shanghai Institute of Optics and Fine Mechanics, Chinese Academy of Sciences, Shanghai 201800, China

### Abstract

**Objective** A 1.5  $\mu$ m pulse fiber amplifier in the eye-safe band is one of the prominent areas of research in pulse fiber laser technology. Depending on the pulse width, fiber amplifiers are used on different occasions; nanosecond fiber amplifiers are used in lidar, and microsecond fiber amplifiers are used in special material processing, biomedicine, and other fields. However, compared with nanosecond fiber amplifiers, the study of high-power microsecond pulsed fiber amplifiers is more challenging because of the steepening of the pulse waveform during amplification and the significantly increase in amplified spontaneous emission (ASE) at low repetition frequencies. In this study, a two-stage master oscillator power amplifier (MOPA) all-fiber structure was used to design and realize a 1550 nm microsecond rectangular pulse fiber amplifier with an adjustable repetition frequency of 10 Hz to 10 kHz. Compared with the fiber amplifier mentioned by M. Yu. Koptev and Svitlana Pavlova, the present one reduced the system complexity and cost and realized a wider range of adjustable repetition frequencies.

**Methods** The entire fiber amplifier consists of four parts: signal optical pulse modulation, preamplifier, power amplifier, and pulse signal driving and control (Fig. 1). The optical signal pulse is modulated by a continuous seed source using an acousto-optic modulator (AOM). The preamplifier consisted of a double-clad erbium-ytterbium co-doped fiber (Nufern, PM-EYDF-12/130, length of 2.4 m), pump laser diode (pump wavelength is 940 nm, maximum optical power of 10 W), multimode pump beam combiner (MPC), and cladding pump stripper (CPS). The power amplifier included a double-clad erbium ytterbium co-doped fiber (Nufern, PM-EYDF-12/130, length 3.8 m), pump laser diode (940 nm, 80 W), MPC, and CPS. Both the preamplifier and power amplifier use the pulse-pump mode. The RF driver of the AOM, preamplifier pump driver, and power amplifier pump driver can be accurately synchronized and controlled, and the pulse width can be adjusted. The AOM operation is used to solve the waveform distortion caused by the narrowing of the pulse width in two different modes. By controlling the timing of the pulse signal and pre-shaping the waveform, the challenges of rapid ASE growth and transient effect of the pulse fiber amplifier are addressed.

**Results and discussions** By setting the pulse timing and pulse width of the AOM RF driver, the preamplifier pump driver, and power amplifier pump driver of the pulse fiber amplifier (Table 2), and optimizing the parameter settings of the AOM to pre-shape the pulse waveform of the input signal light, the output signal optical pulse waveform of the fiber amplifier is made rectangular (Fig. 4). The peak power reached 30 W at different pulse repetition frequencies and widths (Table 3). When the AOM was operated in mode 1, the optical-to-optical conversion efficiency was approximately 34%. Because the timing of the signal light pulse and pump pulse has been optimized to suppress the growth of the ASE, the spectral side-mode suppression ratio is close to 55 dB (Fig. 5), and there is no

ASE generation. When the AOM operates in mode 2, the optical-to-optical conversion efficiency gradually increases from 19.50% to 24.19%. As the pulse repetition frequency continues to increase, the interval between two adjacent pulses becomes shorter, and the ASE accumulation time decreases, which is conducive to an increase in the signal optical power. However, keeping the pulse width constant and increasing the pulse repetition frequency leads to a continuous increase in the pulse duty cycle and number of pulses per unit time, resulting in an increase in the absorbed pump optical energy per unit time. The spectral side-mode suppression ratio is 25 dB. This is because when the pulse width is narrow, and the excess energy of a single pump pulse continues to convert energy between ions. The rapid accumulation of the ASE leads to a decrease in the spectral side-mode suppression ratio.

**Conclusions** A 1550 nm microsecond pulse fiber amplifier with an adjustable repetition frequency of 10 Hz–10 kHz was designed and realized. The fiber amplifier adopts a pulse-pumped all-fiber dual-stage MOPA structure. By setting two working modes of the acousto-optic modulator (AOM), it realizes a working wavelength of 1550 nm, peak output power of 30 W, pulse width of 10  $\mu$ s to 1 ms, and wide range adjustable rectangular pulse repetition frequency of 10 Hz to 10 kHz. In this system, the rapid growth of the ASE is suppressed by optimizing the timing and pulse width of the signal and pump beams. The waveform distortion problem caused by the transient gain effect in microsecond pulse fiber amplification is overcome by pre-shaping the signal optical pulse waveform, and a better rectangular pulse laser output is obtained. A microsecond pulse fiber amplifier has high peak power. The pulse width and repetition frequency of the amplifier can theoretically be adjusted to a wider range. The microsecond pulse fiber amplifier has broad application prospects in laser drilling, laser coloring, and biomedicine.

**Key words** optical devices; optical amplifier; microsecond pulse; erbium-ytterbium co-doped fiber; acousto-optic modulator; master oscillator power amplifier